ASTRONOMY & ASTROPHYSICS
SUPPLEMENT SERIES

Astron. Astrophys. Suppl. Ser. **61,** 93-106 (1985)

The Antlia cluster of galaxies and its environment : the Hydra I-Centaurus supercluster (*)

U. Hopp and J. Materne

Institut für Astronomie und Astrophysik, Technische Universität Berlin/PN 8-1,
Hardenbergstraße 36, D-1000 Berlin 12, F.R.G.

Received July 18, 1984, accepted February 25, 1985

Summary. — The small Antlia cluster of galaxies was investigated by measuring many radial velocities for galaxies from the Lauberts catalogue in the Antlia region. Apart from the Antlia cluster itself, four more small groups were identified. These five systems form a tiny but not bound Antlia mini-supercluster. The mini-supercluster consists of small groups and clusters and of a dispersed component of field galaxies.
The five galaxy systems are also part of the large Hydra I-Centaurus supercluster. This large supercluster belongs now to the class of well observed ones. It has a chain-like filamentary structure. This supercluster seems to be connected to the Local Supercluster *via* two very extended but very loose groups. The total structure is the triangle-shaped Virgo-Hydra I-Centaurus supercluster.

Key words : clusters of galaxies — groups of galaxies — local supercluster — radial velocities — redshifts.

1. Introduction.

The Antlia cluster of galaxies is a beautiful, small, nearby cluster of Bautz-Morgan type III (Sandage, 1975). It is stressed that this cluster as defined by Sandage or Huchra and Geller (1982, their group number 18) is not the same as the Antlia group of Tully (1982). The latter is equal to de Vaucouleurs' (1975) group number 8, which is a small group in the Local Supercluster. The subject of the present article is the Antlia cluster as identified by Sandage. It was assumed to have a mean radial velocity of about 2900 km s^{-1} when some twenty radial velocities of member galaxies were available. An inspection of galaxy surface density distribution revealed that this cluster appeared strongly elongated, a common phenomenon (Binggeli, 1982).

Single clusters and groups of galaxies have been studied for some time but their description is still quite phenomenological (Chincarini, 1980). A detailed dynamical understanding is still lacking for most of them. It is not clear if rotation is important for the cluster dynamics or if the flattening is due to an anisotropic phase space distribution function of the galaxies (Binney, 1982). In the case of e.g. the Coma cluster or A 2029 cluster, the flattening is probably not caused by simple rotation. It seems possible, however, that the elongation of the cluster SC 0316-444 is produced by rotation of the whole cluster (Materne and Hopp, 1983). In addition most — if not all groups and clusters are members of larger aggregates, superclusters.

Only very few of the known superclusters have been investigated in some greater detail, those are mainly the Hercules supercluster (Tarenghi *et al.*, 1979 and 1980), the Perseus supercluster (Gregory *et al.*, 1981), and last but not least the Coma-A 1367 supercluster (Gregory and Tifft, 1976). But in most cases the membership assignment of galaxies or clusters to superclusters is by no means clear. The kinematical or dynamical relations between the contributing clusters are neither known.

As part of a larger investigation, radial velocities were measured of galaxies in the Antlia cluster and its environment. Since the Antlia cluster is a relatively nearby one it is a good object to study the membership assignment of a single galaxy to a cluster as well as the assignments of clusters to possible superclusters. These observations will be presented in section 2. In section 3 we shall deal with the question how to define the groups and clusters which we suspect to exist in that area. We applied the concept developed earlier by Materne (1979) to define and classify the systems in the survey area. The resulting clusters and their properties namely total luminosities and masses are discussed in section 4 while the system of clusters in the survey area as a whole is treated in section 5. The surrounding structure of the supercluster is finally described in section 6.

In the present article a system of galaxies is generally called a cluster of galaxies regardless of its size. Only in the case of a specific system with very few bright member

(*) Based on observations collected at the European Southern Observatory, La Silla, Chile.
Send offprint requests to : J. Materne.

galaxies the expression group of galaxies will be used. Both sorts of systems are supposed to be gravitationally bound. This nomenclature is used in taxonomy or cluster theory where no distinction is made with respect to the size of a system.

2. Observational data.

2.1 THE SAMPLE OF GALAXIES. — The Antlia cluster of galaxies is centered at $10^h27^m - 35°.1$. It has an extension of a few degrees. To obtain a relatively well defined sample of galaxies the observed objects were selected from the Lauberts (1982) catalogue (LC) which is complete for galaxies having a major diameter $2A$ larger than one arcmin and it is almost a magnitude limited sample since magnitudes and diameters correlate. All galaxies between 10^h00^m and 10^h50^m as well as between $-42°$ and $-30°$ were taken into account. This area will be called *Antlia region* further on. There are 258 galaxies. The galaxy distribution on the sky is shown in figure 1. Galaxies with known velocities are plotted with crosses, the others with dots. The galaxy distribution in the larger context can be seen on page 13 of the LC. At 10^h30^m the lump of galaxies near the edge of Lauberts plot is the Hydra I (Abell 1060) cluster, the less pronounced density enhancement near to it, somewhat southern, is the Antlia cluster.

Sadler (1982, 1984) estimated that the LC is probably complete to a magnitude of $B = 14.0$. It will become seriously incomplete only at magnitudes fainter than 16. The classification of morphological types poses, again after Sadler, no problems for galaxies brighter than $B = 14.0$ but is affected for galaxies in the range $14 < B < 16$.

The diameter limit also leads to different limiting magnitudes for S0 and E galaxies (Sadler observed only early type galaxies). This conclusion is supported by figure 2 where the distribution of all the 258 galaxies in the Antlia region with respect to their magnitudes is given. For the determination of the magnitudes see section 2.3.

The 258 galaxies of the Antlia region are listed in table I. The first column contains a running number, the second the NGC or IC number, the third the old ESO identification; then follow the coordinates as given in the LC in columns four and five, the velocities with errors and references (see below) in column six. The types, magnitudes (see below), and the diameters from the LC are listed in columns seven to ten. The last two columns contain the clusters to which the galaxies belong and the membership probabilities (see below).

2.2 THE RADIAL VELOCITIES. — When this investigation was started radial velocities for 32 galaxies (= 8 %) were available in the literature. To get a useful sample, spectra for 69 more galaxies were secured with the Boller & Chivens spectrograph attached to the Cassegrain focus of the ESO 1.52 m telescope and an EMI three stage image tube. A useful spectral range from 3800 Å to 5800 Å was covered by using an inverse linear dispersion of 114 Å mm^{-1}.

All spectra were measured with the ESO Grant machine in Garching. Generally, the absorption lines of Ca II, H and K, Ca I and the *G*-band were used. The Fe 4383 line, the Mg I doublet and the Fe/Ca blend at 5969 Å were often included. In the case of emission line objects [O II] 3728, [O III] N1 and N2, and Hβ were used. The spectra were only exposed for a minimum of time, some five to twenty minutes to get a large sample. The errors in the velocities are in the range $\delta v = 30\text{-}100$ km s^{-1}.

In table I the new, heliocentric, radial velocities are given together with their individual errors as derived from the internal scatter of the individual lines. A total of 101 radial velocities is now available in the Antlia region. In figure 3 the distribution of these radial velocities is presented in form of histogrammes.

For five galaxies (type E, S0) velocities are in common with Sadler (1982). The comparison of the two sets yields as difference $\langle v_{HM} - v_S \rangle = (+59 \pm 90)$ km s^{-1}. There seems to be no significant systematic difference.

2.3 THE LUMINOSITY CALIBRATION. — Out of the 258 galaxies in the Antlia region only 35 had photometric data in the LC. Therefore we were forced to estimate B^* magnitudes for the rest of them. All galaxies from the LC were collected having the same galactic latitude ($b = -25° \ldots -14°$) as the Antlia region, having a photometry accurate to $\delta B \leqslant 0.39$, and having an unambiguous Hubble classification. This gives a total of 113 galaxies. The published B magnitudes were corrected to $B_{T,0}$ magnitudes in the way proposed by Sandage and Tammann (1981) in the Revised Shapley-Ames Catalogue. These corrected magnitudes $B_{T,0}$ were correlated with the logarithm of the squared major diameter by an error weighted linear least square fit. The resulting correlation is

$$B_{T,0} = (18^m.33 \pm 0^m.12) - (1^m.96 \pm 0^m.45) \log \frac{(2A)^2}{\square'} \quad (1)$$

A^2 instead of $A \cdot B$ is taken because the inclination is taken care of. If $A = B$, only the correction remains for absorption of the dust disk in a face-on spiral galaxy. The fit is shown in figure 4. The 1 σ accuracy of our estimated $B^*_{T,0}$ calculated from equation (1) is 35 % in luminosity. They were derived in the usual way

$$\frac{L_B}{L_B^{\odot}} = \left(\frac{v_{rad}}{H_0}\right)^2 \cdot 10^{\frac{B^*_{T,0} - 0.48}{2.5}} \quad (2)$$

where $M_B^{\odot} = 5.48$ and $H_0 = 50$ km s^{-1}/Mpc.

It seems to be surprising that early type galaxies were combined with late type ones. In figure 4, however, the S0 and spiral galaxies mix perfectly and the E galaxies are too few to derive any significant correlation. Numerically no significant difference for the different types could be found. This may be caused partly by the relative high uncertainty of the fit. In table I, all the $B^*_{T,0}$ (or $B_{T,0}$ when available) are given for the galaxies in the Antlia region.

3. Cluster definitions.

3.1 A PRELIMINARY CLASSIFICATION. — The method used here to determine clusters of galaxies was described by Materne (1979). After selecting an initial configuration of clusters, a probability density function was fitted to the galaxy distribution. In the present case, initial configurations were derived in first approximation by inspection of the data, i.e. the positions of all galaxies as given in figure 1 and the velocities which are available as given in figures 3 and 6. As a check a quick run with the hierarchical clustering (Materne, 1977) was performed. No new results emerged. For this small sample — which is not too complex — the intuitive analysis was sufficient.

Tentatively six clusters were identified. One is a background group with seven probable members at $10^h13^m - 35°$ having a mean radial velocity of 8900 km s^{-1}. It covers an area of $2.°0 \times 1.°5$ on the sky, corresponding to 6.2 Mpc × 4.7 Mpc and its velocity dispersion is 370 km s^{-1}. The reality and properties of this group will not be investigated any further in the present article. We shall concentrate on the remaining five systems.

i) The main peak at 2900 km s^{-1} in the velocity distribution (Fig. 3) is due to the galaxies in the Antlia cluster proper which is also pronounced in the centre of figure 1.

ii) A small group around the galaxy NGC 3244 at the same radial velocity as the Antlia cluster is south to it but clearly separated.

iii) West of these two clusters a third group is centered on the galaxy ESO 316-G43. It mainly causes the second peak at 4800 km s^{-1} in the velocity histogramme (Fig. 3).

iv) Also west to the Antlia cluster but at a mean radial velocity similar to the one of the Antlia cluster is a loose density enhancement around the galaxy IC 2558.

v) Finally, one can probably identify east of Antlia a small group around the galaxy NGC 3333. Most of the members have high velocities, similar to the ones in the ESO 316-G43 group.

In addition to these clusters, we draw the attention to the galaxies north of the Antlia cluster with radial velocities similar or slightly higher than the ones in the cluster. At the northern boundary of the survey region these galaxies form apparently a connection to the Hydra I cluster (Richter, 1982). The latter has a radial velocity only slightly higher than the Antlia cluster (v_{Hya} = 3400 km s^{-1}). We shall come back to this point in section 6.

3.2 THE PROBABILITY DENSITY FUNCTION. — The coarse classification derived above gives the possibility to fit a probability density function (pdf) to the galaxy distribution on the sky and in velocities. The method of Materne (1979) was adopted. At that time for reasons of simplicity a Gaussian distribution was selected for the radial projected density distribution and for the distribution of velocities. The larger sample here allows some experimentation with other distribution functions as well.

The pdf $\phi(\mathbf{r})$ is split into a background term ϕ_b and a cluster term ϕ_{cl}^{ν} for the ν^{th} cluster :

$$\phi(\mathbf{r}) = \phi_b(\mathbf{r}) + \sum_{\nu}^{k} \phi_{cl}^{\nu}(\mathbf{r}), \tag{3}$$

where $\mathbf{r}$ stands for generalized coordinates (here positions at the sky and radial velocities). For a more detailed discussion see Materne (1979).

For simplicity the summation over ν, the clusters, will be dropped in the following, i.e. only isolated clusters are treated. In practice, of course, fits for several clusters have to be done simultaneously. A constant density is adopted for the background, this is only an approximation because our sample is magnitude limited and this causes the density to decrease with increasing distance. Then the background distribution can be written as :

$$\phi_b(\mathbf{r}) = \frac{3\, v^2}{A_{sky} \cdot v_{max}^3}\left(1 - \frac{\mu}{N}\right) \tag{4}$$

with

A_{sky} the survey area at the sky (here solid angle on the sky)
v velocity for which ϕ is to be evaluated (v is part of the generalized coordinate $\mathbf{r}$)
μ number of galaxies in the cluster
N number of galaxies in the sample
v_{max} velocity depth of the sample (5700 km s^{-1}).

The terms A_{sky} and $1/3\, v_{max}^3$ form the normalization of the pdf and $\left(1 - \frac{\mu}{N}\right)$ is the fraction of galaxies belonging to the background. Because of the homogeneous distribution on the sky, the positions do not show up. In depth, however, the metric surface area of the cone, given by A_{sky}, increases with v^2.

It will be further assumed that galaxy positions are independent of their velocities. Then

$$\phi_{cl}(\mathbf{r}) = \phi_{cl}(\alpha, \delta) . \phi_{cl}(v) . \tag{5}$$

For the velocity distribution $\phi_{cl}(v)$ a Maxwellian distribution projected along the line of sight is taken (Yahil and Vidal, 1977) :

$$\phi_{cl}(v) = \frac{(\mu/N)^{1/3}}{(2\,\pi)^{1/2}\,\sigma_v} \exp - \frac{(v - \bar{v})^2}{2\,\sigma_v^2} \tag{6}$$

with

$\bar{v}$ mean velocity of the cluster
σ_v velocity dispersion of the cluster (size in velocity space).

For the positional distribution $\phi_{cl}(\alpha, \delta)$ we tried several possibilities :

i) A circular symmetrical Gauss distribution (CG-model)

$$\phi_{cl}^{CG}(\alpha, \delta) = \frac{(\mu/N)^{2/3}}{2\,\pi\sigma_{ab}^2} \exp\left[- \frac{(\alpha - \bar{\alpha})^2}{2\,\sigma_{ab}^2} - \frac{(\delta - \bar{\delta})^2}{2\,\sigma_{ab}^2} \right] \tag{7}$$

with

$\bar{\alpha}, \bar{\delta}$ the mean position of the cluster
σ_{ab} the size (positional dispersion) of the cluster as in Materne (1979).

ii) A modified Hubble distribution (CM-model)

$$\phi_{cl}^{CM}(\alpha, \delta) = \frac{(\mu/N)^{2/3}}{2\,\pi\sigma_{ab}^2(1 + A_{sky}/\sigma_{ab}^2)^{1/2}} \cdot \left[1 + \frac{(\alpha - \bar{\alpha})^2 + (\delta - \bar{\delta})^2}{\sigma_{ab}^2} \right]^{-1/2} . \tag{8}$$

This leads to a spatial density distribution of

$$\rho \sim \left[1 - \left(\frac{r}{s_0}\right)^2\right]^{-1} \tag{9}$$

which is often used for gas density analysis from X-ray observations, cf. the recent discussion by Steward *et al.* (1984) and references therein. Properties of the function ϕ^{CM} were discussed by Fuchs and Materne (1982).

iii) A two dimensional Gauss fit (EG-model)

$$\phi_{cl}^{EG}(\alpha, \delta) = \frac{(\mu/N)^{2/3}}{2\,\pi\sigma_{ab}} \cdot \exp\left\{ - \frac{[(\alpha - \bar{\alpha}) \cos \chi + (\delta - \bar{\delta}) \sin \chi]^2}{2\,\sigma_a^2} - \frac{[(\alpha - \bar{\alpha}) \sin \chi - (\delta - \bar{\delta}) \cos \chi]^2}{2\,\sigma_b^2} \right\} \tag{10}$$

with σ_a and σ_b major and minor axis of the cluster position, χ angle (it is counted from north counterclockwise).

The results can be summerized in the following way :

i) The five above identified systems are well separated. Therefore, only very few test runs were necessary dealing with several clusters simultaneously and it was generally sufficient to treat the clusters isolated.

ii) The assumption of projected Gaussian density distributions gave always the most stable fits.

iii) The CM-model puts very much weight onto the velocities. The scale length for the velocities and for the extend at the sky are not equivalent. The CM-model always finds groups with narrow velocity distribution but very broad distributions at the sky.

iv) Already a visual inspection shows that the clusters are not circular but elongated. Therefore, the EG-model was finally adopted. It gave indeed very satisfactory results.

3.3 THE RESULTING GROUPS AND CLUSTERS. — The main results derived in the following are based on the EG-model (Gaussian and elongated distribution). In the last but one column of table I the groups are given to which the galaxies belong and in the very last the membership probabilities in percent.

The pdf gives the membership assignment and other basic group parameters which have been listed in table II for the EG-model. For the Antlia cluster two solutions were possible. The central part is called Antlia II. This is the Antlia cluster proper. Another fit, however, is possible for the pfd, we call it the Antlia I cluster. It covers a larger area on the sky. Most of the galaxies of the IC 2558 group and of the galaxies being foreground to the NGC 3333 group are included in Antlia I. This was the only case where the isolated cluster fit and the multicluster fit gave different results. A possible physical interpretation will be discussed below.

The errors of the fitted parameters are typically 0°.1 for the positions, 0°.2 for the sizes, 100 km s^{-1} for the mean velocities, a little less for the velocity dispersions, the position angle is rather uncertain, 20°, and the number is uncertain by one to five, typically 10 % to 20 %.

For all the clusters two solutions were derived, one including only galaxies with measured radial velocities, the other including all galaxies of the sample. Generally, the pdf fit added galaxies without velocities only to a cluster in question if the galaxies were projected directly onto the cluster. Therefore, the inclusion of galaxies without velocities increases the number of members only for the Antlia II cluster and for the NGC 3244 group significantly because several galaxies without measured velocities are projected onto them.

4. Dynamical group properties.

The inspection of the velocity distribution of the galaxies in the Antlia cluster shows no significant pattern. No indication is seen that the Antlia cluster maintains its elongation by rotation. This result cannot be caused by the selection procedure for the member galaxies, there are too few galaxies projected onto the cluster which are deleted as non-Antlia members by the pdf.

4.1 THE TYPES. — Lauberts (1982) estimated the morphological types of the catalogued galaxies. The clusters discussed here consist mostly of late type galaxies. This can be seen in figure 5 where the type distribution of the sample galaxies is plotted. The distribution of types onto the individual clusters is shown in table III. Two remarks seem appropriate regarding table III : i) the absolute number of galaxies for each type is very small. Therefore, the statistics is rather unreliable. ii) The sum over the types may give higher numbers for a cluster in table III than the numbers in table II. The reason is that in table III each fractional member was counted as a full member while in table II the fractions are summed by the pdf.

In clusters the E/S0 galaxies have a steeper density gradient than the spiral galaxies (Dressler, 1980). For the three clusters Antlia, NGC 3244, and ESO 316-G43 there are probably enough galaxies to see whether this is the case. In table IV the mean distances $\langle r \rangle$ of the galaxies to the cluster centres are given where the galaxies are sorted into early and late types. As far as the coarse results can be interpreted, we find that the early type galaxies indeed tend to form the core while the late type ones form a somewhat broader halo.

Moles and Nottale (1981) using the redshifts of Sandage (1975) found a substantial difference in the Antlia cluster for the radial velocities of the early type and the late type galaxies respectively : $\langle v_{E/S0} \rangle - \langle v_s \rangle = (714 \pm 254)$ km s^{-1}. We have now many more velocity measurements and find

$$\langle v_{E/S0} \rangle = (2718 \pm 171)\ \text{km s}^{-1} \quad \text{dispersion } 591\ \text{km s}^{-1} \tag{11a}$$

$$\langle v_S \rangle = (3058 \pm 140)\ \text{km s}^{-1} \quad \text{dispersion } 444\ \text{km s}^{-1}\,. \tag{11b}$$

The two types have — within the errors — practically the same radial velocities. And, contrary to the Virgo cluster (Sandage and Tammann, 1976; Ftaclas *et al.*, 1984), the two types have also similar velocity dispersions.

4.2 LUMINOSITIES. — The luminosities of the galaxies were taken from table I. For each group these luminosities were summed using as weights the membership probabilities. All galaxies, also those without measured radial velocities, were included with their appropriate membership probabilities. This should give the best estimates for the total observed cluster luminosity. It still has to be corrected for the luminosities of the faint galaxies not included in LC. Using the integrated Schechter luminosity function we get $L_{tot}/L_{obs} = \Gamma(\alpha+2)/\Gamma(\alpha+2, L_{lim}/L_*)$. As parameters we took $\alpha = -1.25$, L_* from $M_* = -20.6$ and from figure 4 we estimated the limiting magnitude to be 14.5 which gives at each group the appropriate L_{lim}. The corrected cluster luminosities are given in table V. We note that the solution for Antlia I (large, extended system) gives more than three times as much luminosity as the solution for Antlia II (the compact, central part).

4.3 MASSES. — For the mass estimates of the clusters the virial theorem is used in the simple form

$$\mathcal{M}_{vir} = \frac{R_{vir} \cdot \langle \sigma_v^2 \rangle}{G} \quad (12)$$

with

R_{vir} virial radius of the cluster

$\langle \sigma_v^2 \rangle$ the mean relative velocity of the member galaxies squared, i.e. the velocity dispersion, corrected for observational errors (Materne, 1974).

Both have to be corrected for projection effects.

4.4.1 *Virial radius.* — The virial radius R_{vir} — being the harmonic mean of the galaxy-galaxy distance — was calculated by evaluating the sum

$$R_{vir}^{-1} = \frac{1}{N^2} \sum_{i,j} \frac{1}{r_{ij}}. \quad (13)$$

In table VI two values for each cluster are given : the virial radius in degrees as projected on the sky, i.e. no correction for projection effects are made and the virial radius in Mpc fully corrected for projection effects according to Limber and Mathews (1960). The radii in degrees can be compared with the results calculated by the pdf.

In the summation of equation (13) the galaxies were included with respect to their membership probabilities. To make the summation procedure fast, the number of members according to table II were taken and all galaxies with decreasing membership probabilities included so that the total number was reached. This neglects somewhat galaxies with very low membership probabilities but because these probabilities are very small, the errors introduced this way are small as well (a few percent).

4.4.2 *Crossing time.* — An important test if small clusters of galaxies are physically bound or just chance projections is the relation of the crossing time to the age of the universe (Field and Saslaw, 1971; Turner and Sargent, 1974). The crossing time T_{cr} is calculated by

$$T_{cr} = 2\, R_{vir} \langle \sigma_v^2 \rangle^{-1/2}. \quad (14)$$

For the virial radius the values of table V were taken. The mean velocities and the velocity dispersion given in table V were calculated from the member galaxies of each cluster weighed with the corresponding membership probability. The correction for observational errors causes the velocity dispersion of table V to be lower than the ones given by pdf in table II.

Surprisingly small are the velocity dispersions for the two clusters NGC 3244 and NGC 3333. They lead to crossing times larger than the Hubble time, cf. table V. We always felt a bit uncertain about the NGC 3333 group. Only three radial velocities of galaxies relatively far apart from each other are available. The results for the NGC 3244 group we do not understand, however, because it appears as relatively isolated group with member galaxies all having appropriate radial velocities.

The problem encountered here is that any algorithm to define groups and clusters in a three dimensional way tends to reduce the velocity dispersion. But physically bound systems need a certain amount of velocity dispersion to counteract the gravitational force. In systems with small membership numbers this may lead to unresolvable conflicts.

4.4.3 *Virial masses.* — With the results derived so far, the virial mass for each cluster can be calculated and have been listed in table V. The mass of a few times $10^{14}\ \mathcal{M}_\odot$ for the Antlia cluster is much higher than the masses of the nearby small groups of galaxies (Materne, 1980).

The mass-to-light ratios can be calculated now as well. They are given in the final column of table V. The small mass-to-light ratio for the extended Antlia I system compared with the Antlia II system has mainly two reasons. i) Antlia I has a higher total luminosity, many more galaxies are included. ii) Antlia I has a lower velocity dispersion, the galaxies seen in the vicinity of Antlia I are only included if their radial velocities are very similar to the mean radial velocity of Antlia I. If Antlia I were the correct solution, we would observe the case of a strong anisotropic velocity distribution, the velocities are directed mainly to the cluster centre. In the centre of the cluster we see the high velocity dispersion as indicated in Antlia II while the outlying members (in projection) have mainly velocity components perpendicular to the line of sight.

In summary, one can say that the mass-to-light ratios of the groups and clusters in the Antlia region have the uncomfortable high values mostly found in groups and clusters of galaxies.

5. The system of clusters in the Antlia region.

In addition to the distribution of galaxies on the sky as shown in figure 1, the distribution in depth is given in figure 6. The velocity dispersion of the clusters are indicated by vertical bars and the sizes resulting from the pdf by horizontal ones. In this case the results from the CG-model (one dimensional Gauss distribution) was used because the chosen χ-axis — the angle at the sky — is inclined by forty degrees against the δ-axis. As a consequence the Antlia cluster and the NGC 2558 group overlap but all the others are well separated.

The pdf fit found and separated the different clusters easily. We draw attention to the fact, however, that regardless of the projection the clusters do not appear fully isolated. One has the impression of a dispersed component of galaxies with superimposed density enhancements, the clusters. Such a dispersed component was already described by Tarenghi *et al.* (1979, 1980) and Materne *et al.* (1980) for the Hercules supercluster.

Figures 1 and 6 show that the dispersed component is not only between the clusters but extends also northwards to the Hydra I cluster (Richter, 1982; Richter *et al.*, 1982). This is what we mean by « bridge » in figure 6. The much larger system including the Hydra I cluster will be discussed in the next paragraph.

The system of the five clusters in the Antlia region is relative compact. A check was performed to determine whether it is gravitationally bound. In this case the clusters were treated as mass points with masses as given in table V. Virialization seems not to be a very sensible assumption for this system of five « mass points ». Therefore, the concept of Materne (1974) was used and the potential energy as well as kinetic energy T was calculated. The system would be bound (but not necessarily relaxed) if $T + \Omega = 0$ or $T/\Omega \leqslant 1$. We find for the systems in the Antlia region $T/\Omega \leqslant 5.4$ so that this system of galaxy clusters is not gravitationally bound. If, however, the two background groups NGC 3333 and ESO 316-G43 are excluded we get $T/\Omega = 0.11$.

6. The Hydra-Centaurus supercluster.

6.1 THE SUPERCLUSTER. — Chincarini and Rood (1979) discovered the Hydra I-Centaurus supercluster on the basis of the ScI galaxy distribution. The small separation between the Antlia region and the Hydra I cluster, the similarity of the radial velocities of three of the Antlia region clusters to the velocity of the Hydra I cluster (Richter, 1982; Richter *et al.*, 1982) made us look at the larger system Hydra I-Centaurus again.

In addition to the clusters discussed above, the Hydra I-Centaurus system contains many more clusters several of which were already identified by Sandage (1975). Their mean positions, mean velocities, velocity dispersions and prominent members are given in table VI. To see that these clusters really form a supercluster, the positions of all the known clusters with their sizes are plotted in figure 7. The parameters for these member clusters are only coarse calculations because a detailed investigation of all the members of the Hydra I-Centaurus supercluster is beyond the scope of the present paper. It can be seen that this supercluster has two prominent subsystems, the Centaurus and the Hydra I-Antlia cluster. The structure is possibly even more complex if the results of Lucey *et al.* (1984) are taken into account : the Centaurus cluster has a bimodal velocity distribution.

Apart from the member clusters we found five field galaxies which form sort of a connection between the two subsystems. These five galaxies are ESO 378-G3, NGC 3706, NGC 4783, ESO 378-G20, and IC 2977. They are plotted as dots in figure 7. The whole supercluster has a chain-like appearance. It may be one of the filamentary structures as discussed by Jôeveer and Einasto (1978). The chain is not a chance projection as can be seen in the diagram velocity *versus* angle at the sky in figure 8. The two background groups in the Antlia region seem to be, however, somewhat detached. Again the five field galaxies indicate a connection.

The galaxy NGC 4936 at $13^h01^m\!.5 - 30°15'$ with a radial velocity of 3309 km s^{-1} is not plotted. This dominant E galaxy has some twelve companions (Sandage, 1975) and may form a connection between the ESO 508-G19 group and the Centaurus cluster proper.

6.2 CONNECTIONS TO THE LOCAL SUPERCLUSTER. — In order to understand better the Hydra I-Centaurus supercluster we looked at all galaxies of the LC which have known radial velocities in the region $10^h \leqslant R.A. \leqslant 14^h$ and $-40° \leqslant Dec. \leqslant -17\overset{\circ}{.}5$. Apart from the known members of the supercluster, we found (among others) two large but loose groups with radial velocities of about 1500 km s^{-1}. One covers the region 11^h50^m to 12^h00^m and $-30°$ to $-17\overset{\circ}{.}5$. Its southern part is in fact formed by de Vaucouleurs (1975) group 44. The other covers the region 13^h10^m to 13^h30^m and $-30°$ to $-17\overset{\circ}{.}5$, the southern part may even extend further south. In both cases the northern edge is given by the catalogue limits.

If these two galaxy systems are really bound groups or clusters of galaxies situated at the distance as indicated by the radial velocities, they have remarkable properties. They are strongly elongated in north-south direction, they are very large, about 8 Mpc × 3 Mpc, and they are very loose.

The radial velocities indicate distances which are approximately half way between the Hydra I-Centaurus and our Local Supercluster. They may form a filamentary connection between the Local Supercluster and the Hydra I-Centaurus supercluster. Indeed, we should speak about the Virgo-Hydra I-Centaurus supercluster.

The influence of these large clusters can also be seen in the motion of the Local Group relative to these clusters. Tammann (private communication), see also Shaya (1984), claims that the Local Group moves in a direction half way between the Virgo cluster and Hydra I-Centaurus supercluster. Furthermore, Tully (1982) has shown that the Local Supercluster has its longest axis pointing towards the Hydra I-Centaurus supercluster.

7. Conclusion.

A system of five small clusters of galaxies centered in the Antlia cluster was investigated. These five clusters are close together being imbedded in a dispersed component of galaxies. They are normal small groups or clusters with the well known discrepancy of mass-to-light ratios of more than a hundred solar units. There is presently no indication that these five systems form a gravitational bound system in spite of the fact they are so close to each other.

The five clusters are part of the Hydra I-Centaurus supercluster. Many positions and radial velocities are available for galaxies in this supercluster. It is now nearly as well investigated as are the Coma-A 1367 (Gregory and Tifft, 1976) supercluster, the Perseus supercluster (Gregory *et al.*, 1981), and the Hercules supercluster (Tarenghi *et al.*, 1979 and 1980). The Hydra I-Centaurus supercluster resembles a chain-like structure. Two concentrations, the Hydra I and the Centaurus cluster, are connected by a bridge consisting of small clusters and individual galaxies.

There are strong indications that at least two filaments reach from this bridge to the Local Virgo Supercluster. In this case, it is an advantage that we as observers are situated inside this large system since we can delineate its internal structure. It contains at least three rich clusters of galaxies forming sort of a triangle, the Virgo-Hydra I-Centaurus supercluster.

Acknowledgements.

Andris Lauberts put unpublished data at our disposal. We are very grateful to the European Southern Observatory for the allotment of observing time on La Silla and for giving us the possibility to reduce the data efficiently in Garching. Guido Chincarini gave very valuable advices at different stages of the manuscript.

References

BINGGELI, B. : 1982, *Astron. Astrophys.* **107,** 338.
BINNEY, J. J. : 1982, in *Morphology and Dynamics of Galaxies,* eds. L. Martinet and M. Mayor (Swiss Society of Astronomy and Astrophysics, Geneva Observatory).
CHINCARINI, G. : 1980, in *X-ray Astronomy,* Proc. of the NATO Advanced Study Institute, Erice, July 1-14, 1979, eds. R. Giacconi and G. Setti (Reidel Publishing Company).
CHINCARINI, G. and ROOD, H. J. : 1979, *Astrophys. J.* **230,** 648.
DAWE, J. A., DICKENS, R. J. and PETERSON, B. A. : 1977, *Monthly Notices Roy. Astron. Soc.* **178,** 675.
DRESSLER, A. : 1980, *Astrophys. J.* **236,** 351.
EINASTO, J., JÔEVEER, M. and SAAR, E. : 1980, *Monthly Notices Roy. Astron. Soc.* **193,** 353.
FIELD, G. B. and SASLAW, C. W. : 1971, *Astrophys. J.* **170,** 199.
FTACLAS, C., FANELLI, M. N. and STRUBLE, M. F. : 1984, *Astrophys. J.* **282,** 19.
FUCHS, B., MATERNE, J. : 1982, *Astron. Astrophys.* **113,** 85.
GREGORY, S. A., THOMPSON, L. A. and TIFFT, W. G. : 1981, *Astrophys. J.* **243,** 411.
GREGORY, S. A. and TIFFT, W. G. : 1976, *Astrophys. J.* **206,** 934.
HUCHRA, J. P., GELLER, M. J. : 1982, *Astrophys. J.* **257,** 423.
HUCHTMEIER, W. K., RICHTER, O.-G., BOHNENSTENGEL, H.-D. and HAUSCHILDT, M. : 1983, *ESO preprint* **250.**
JÔEVEER, M. and EINASTO, J. : 1978, in « The Large Scale Structure of the Universe », *IAU Symp.* 79, Tallinn, Sept. 12-16, 1977, eds. M. S. Longair and J. Einasto (Reidel Publishing Company).
KLEMOLA, A. R. : 1969, *Astron. J.* **74,** 804.
LAUBERTS, A. : 1982, *The ESO/Uppsala Survey of the ESO (B) Atlas* (European Southern Observatory) (LC).
LIMBER, D. N. and MATHEWS, W. G. : 1960, *Astrophys. J.* **132,** 286.
LUCEY, J. R., CURRIE, M. J., DICKENS, R. J. and DAWE, J. A. : 1984, preprint.
MATERNE, J. : 1974, *Astron. Astrophys.* **33,** 451.
MATERNE, J. : 1977, *Astron. Astrophys.* **63,** 401.
MATERNE, J. : 1979, *Astron. Astrophys.* **74,** 235.
MATERNE, J. : 1980, *Astron. Astrophys.* **86,** 91.
MATERNE, J., CHINCARINI, G., ROOD, H. J., TARENGHI, M. and THOMPSON, L. A. : 1980, *Astrophys. J.* **235,** 736.
MATERNE, J. and HOPP, U. : 1983, *Astron. Astrophys.* **124,** L13.
MOLES, M., NOTTALE, L. : 1981, *Astron. Astrophys.* **100,** 258.
QUINTANA, H. and LAWRIE, D. G. : 1982, *Astron. J.* **87,** 1.
RICHTER, O.-G. : 1982, thesis, Universität Hamburg.
RICHTER, O.-G. : 1984, *Astron. Astrophys. Suppl. Ser.* **58,** 131.
RICHTER, O.-G., MATERNE, J. and HUCHTMEIER, W. : 1982, *Astron. Astrophys.* **111,** 193.
SADLER, E. M. : 1982, thesis, Australian National University.
SADLER, E. M. : 1984, *Astron. J.* **89,** 23.
SANDAGE, A. : 1975, *Astrophys. J.* **202,** 563.
SANDAGE, A. and TAMMANN, G. A. : 1976, *Astrophys. J. Lett.* **207,** L1.
SANDAGE, A., TAMMANN, G. A. : 1981, *A Revised Shapley-Ames Catalog of Bright Galaxies* (Carnegie Institution of Washington).
SHAYA, E. J. : 1984, *Astrophys. J.* **280,** 470.
STEWARD, G. C., CANIZARES, C. R., FABIAN, A. C., NULSEN, R. E. J. : 1984, *Astrophys. J.* **278,** 536.
TARENGHI, M., CHINCARINI, G., ROOD, H. J. and THOMPSON, L. A. : 1980, *Astrophys. J.* **235,** 724.
TARENGHI, M., TIFFT, W. G., CHINCARINI, G., ROOD, H. J. and THOMPSON, L. A. : 1979, *Astrophys. J.* **234,** 793.
TULLY, R. B. : 1982, *Astrophys. J.* **257,** 389.
TURNER, E. L. and SARGENT, W. L. W. : 1974, *Astrophys. J.* **194,** 587.
DE VAUCOULEURS, G. : 1975, in *Stars and Stellar Systems IX,* eds., A. Sangade, M. Sandage, J. Kristian (University of Chicago Press) p. 557.
YAHIL, A. and VIDAL, N. V. : 1977, *Astrophys. J.* **214,** 347.

TABLE I. — *Data of all ESO/Uppsala galaxies in the Antlia survey field.*

ID	NGC/IC	ESO-No.	Alpha (1950)			Delta		Rad.Vel.	Ref.	Type	Mag.	2A	2B	Cluster	Probab.
			h	m	s	°	'	[km/s]				[arc	sec]		[%]
1		316-G17	10	0	15	-38	18.2			Sa	14.2	11	3		
2	N3108	435-G32	10	0	16	-31	26.1	2678+/- 23		S0	12.0	40	25		
3		374-G23	10	0	38	-33	42.6			S0	14.1	12	3		
4		374-G24	10	0	48	-33	54.7			Sc	14.2	11	9		
5		316-G20	10	1	10	-38	35.5	12597+/- 33		Sa	14.4	10	8		
6		374-G25	10	1	15	-37	9.1	6980+/- 96	1	Sb	14.1	12	10		
7	I2536	374-G26	10	1	18	-33	42.5	5384+/-106		Sb-c	12.9	24	5		
8	I2538	374-G27	10	1	45	-34	33.9	8412+/- 32		Sc	13.2	20	11		
9	I2539	435-G34	10	2	3	-31	7.1			Sb	13.1	22	6		
10		316-G21	10	2	21	-41	10.4			Sc	12.3	35	4		
11		374-G28	10	2	25	-37	5.4	5061+/- 67		Sa-b	13.7	15	7		
12		435-G36	10	2	36	-31	56.1			S..	14.4	10	5		
13		435-G37	10	2	52	-30	30.9			S..	14.4	10	1		
14		435-G38	10	3	2	-30	38.8			S..	14.2	11	8		
15	N3120	374-G29	10	3	11	-33	58.6			Sc	12.7	28	20		
16		374-G30	10	3	30	-36	50.6	4865+/- 87		Sb-c	14.0	13	6		
17		374-G31	10	3	31	-33	20.1			SBc	12.0	12	9		
18		316-G22	10	3	43	-41	28.3			Sc	13.2	20	10		
19		316-G24	10	3	53	-41	4.5			Sc	14.2	11	2		
20	I2546	374-G32	10	3	53	-33	38.5	10267+/- 86		2x S..	14.4	10	7		
21		316-G25	10	4	17	-41	42.9			S0	14.8	8	3		
22		374-G33	10	4	17	-37	20.3			Sc	14.2	11	10		
23		374-G34	10	4	22	-32	36.7	8775+/- 27		SBa	14.4	10	9		
24		435-G42	10	4	45	-30	12.6			double	14.8	8	3		
25		374-G35	10	4	48	-34	6.7			Sc	13.6	16	3		
26	I2546	374-G36	10	4	53	-33	1.0			2x E	14.2	11	8		
27		316-G28	10	5	8	-39	42.1			S0-a	14.2	11	6		
28		316-G29	10	5	40	-41	5.3			Sa-b	13.1	22	8		
29	I2548	374-G37	10	5	44	-34	59.1	4719+/- 84		SBc	12.8	25	23		
30		435-G44	10	6	12	-30	45.0			Sc	14.0	13	1		
31		435-G45	10	6	20	-30	38.1			dwarf	14.1	12	4		
32		316-G30	10	6	33	-39	50.9			Sa	14.2	11	6		
33		374-G38	10	6	40	-32	32.2			E-S0	15.6	5	3		
34		435-G46	10	6	41	-30	9.1			Sa	14.1	12	5		
35		316-G32	10	6	57	-38	9.8	4845+/- 32	1	S..	13.4	18	12	ESO 316-G43	65
36		316-G33	10	6	59	-38	8.9	4512+/- 0	1	S0	14.0	13	8	ESO 316-G43	74
37		316-G34	10	7	31	-39	41.5			S0	13.8	14	11		
38		316-G35	10	7	34	-40	57.2			S0-a	14.2	11	8		
39		316-G36	10	7	44	-38	12.1	4168+/- 60		Irr	13.8	14	10	ESO 316-G43	51
40		374-G39	10	7	47	-37	3.2			Sc	14.4	10	2		
41		316-G37	10	7	57	-38	36.8			Irr	14.4	10	2		
42		316-G38	10	7	59	-37	53.1	4969+/- 29		Sa	13.8	14	12	ESO 316-G43	56
43		316-G39	10	8	0	-40	40.5			Sb	14.4	10	5		
44		316-G40	10	8	12	-37	47.0	4137+/- 53		S0-a	14.2	11	6	ESO 316-G43	33
45		316-G41	10	8	20	-39	45.9			Sc	14.2	11	1		
46		316-G42	10	8	21	-38	53.8	5685+/- 45		SB0	13.5	17	13		
47		316-G43	10	8	27	-38	14.5	4802+/-128		Sm	13.7	15	15	ESO 316-G43	65
48	I2552	374-G40	10	8	34	-34	35.9	3114+/- 16		S0	13.7	15	15	IC 2558	29
49		435-G50	10	8	35	-30	10.6			Sc	13.1	21	1		
50		316-G44	10	8	54	-39	26.8			Sa	13.7	15	8		
51		316-G45	10	9	12	-40	53.4			S0-a	14.0	13	3		
52	N3157	435-G51	10	9	28	-31	23.7			Sc	12.5	30	8		
53		316-G45	10	9	31	-37	40.7	4700+/- 53		S0-a	14.4	10	7	ESO 316-G43	51
54		374-G41	10	9	41	-37	21.8			S..	14.1	12	6		
55		316-G47	10	10	0	-38	38.2	5295+/- 4		Sb	13.6	16	15		
56		316-G48	10	10	12	-37	58.1			S..	14.4	10	3	ESO 316-G43	52
57	I2556	374-G42	10	10	25	-34	28.9	2351+/- 16		Sc	12.7	27	13	IC 2558	78
58		316-G49	10	10	45	-39	1.3			dwarf	14.1	12	4		
59		374-G43	10	10	47	-34	35.1			E	14.4	10	5	IC 2558	25
60		374-G44	10	11	8	-35	44.1	8521+/- 18		SBa-b	13.8	14	10		
61		317-G 2	10	11	9	-39	35.8			S..	14.4	10	3		
62		317-G 3	10	11	17	-37	57.0	4819+/- 71		S0	14.4	10	8	ESO 316-G43	63
63		374-G45	10	11	30	-34	36.6	4477+/- 30		E	14.1	12	8		
64		374-G45	10	11	30	-34	36.6	4302+/- 52		S0	14.1	12	8		
65		374-G46	10	11	49	-34	53.5	9326+/- 51		E	14.2	11	7		
66		374-G46	10	11	49	-34	53.5	8853+/- 79		E	14.2	11	7		
67		374-G47	10	12	0	-33	59.9			Sc	14.1	12	1	IC 2558	50
68	I2558	375-G 1	10	12	31	-34	5.4	2573+/- 12		Irr	14.4	10	6	IC 2558	91
69	I2559	375-G 2	10	12	32	-33	48.7	2899+/- 22		Sb	13.0	23	10	IC 2558	88
70		317-G 5	10	12	38	-39	33.5			Sa	14.4	10	10		
71		317-G 6	10	12	39	-37	56.4	4529+/- 69		S/Irr	13.8	14	5	ESO 316-G43	37
72		375-G 3	10	13	40	-33	51.9			dwarf	13.5	17	5	IC 2558	36
73		317-G 7	10	13	52	-41	18.4			Sc	14.1	12	7		
74	I2560	375-G 4	10	14	5	-33	18.9	2852+/- 25		Sb	12.0	40	30	IC 2558	65
75		317-G 8	10	14	19	-41	59.8			Sa	13.8	14	11		
76		317-G 9	10	14	53	-38	12.8			S..	14.8	8	5		
77		436-G 8	10	14	53	-31	24.3			S..	14.4	10	10		
78		375-G 5	10	15	11	-36	59.5			dwarf	14.4	10	7		
79		375-G 6	10	15	35	-33	40.2			2x S..	14.1	12	6	IC 2558	4
80		317-G10	10	15	40	-39	38.4			S..	13.7	15	4		
81	I2563	436-G 9	10	16	36	-32	20.8			S..	14.4	10	4		
82		375-G 7	10	16	50	-37	25.2	4833+/- 47		S0	13.8	14	4	ESO 316-G43	40
83		317-G12	10	17	21	-39	13.6			Sb	14.1	12	3	NGC 3244	4
84		436-G10	10	17	31	-31	4.2			Sc	14.1	12	1		

TABLE I *(continued)*.

ID	NGC/IC	ESO-No.	Alpha (1950)			Delta		Rad.Vel.	Ref.	Type	Mag.	2A	2B	Cluster	Probab.
			h	m	s	o	'	[km/s]				[arc	sec]		[%]
85		317-G13	10	17	52	-37	44.8			Sb	14.4	10	2		
86		317-G14	10	18	15	-40	9.0			S0	14.4	10	10		
87		375-G 8	10	18	15	-35	47.0			dwarf	14.2	11	9		
88		317-G15	10	18	18	-39	6.1			Sa	14.2	11	5	NGC 3244	6
89		317-G16	10	18	32	-37	31.6	7633+/- 20	1	Sb	14.0	13	11		
90		375-G 9	10	18	56	-37	14.4			Sc	14.4	10	1	ANTLIA	2
91		375-G10	10	19	0	-33	46.9			Sc	14.1	12	2		
92		317-G17	10	19	8	-39	32.9	2841+/- 35		Sa	13.4	18	12	NGC 3244	58
93	I2570	375-G11	10	19	19	-33	22.1			Sc	14.4	10	6		
94	N3223	375-G12	10	19	21	-34	0.8	2900+/- 8	1	Sc	11.8	46	30		
95	N3224	375-G13	10	19	27	-34	26.6	3101+/- 38		E	13.8	14	12		
96		375-G14	10	19	50	-36	43.2			Sb	14.0	13	2		
97		375-G15	10	20	18	-36	43.6			Sb	14.4	10	4		
98		375-G16	10	20	47	-32	42.0			Sm	14.0	13	6		
99		317-G19	10	20	51	-38	54.8	2833+/- 30		Sa	13.7	15	12	NGC 3244	89
100		317-G21	10	20	57	-39	22.2	2635+/-108		S0	14.0	13	10	NGC 3244	83
101	I2573	375-G17	10	21	16	-35	12.1			Sd	13.2	20	4		
102		317-G22	10	21	23	-38	24.1			Sb	13.6	16	14		
103		375-G18	10	21	27	-35	34.3			S..	14.4	10	4		
104	N3241	436-G16	10	22	1	-32	13.7	2874+/-148	1	Sa	12.7	28	20		
105		375-G19	10	22	7	-33	5.2			S..	14.4	10	8		
106		375-G20	10	22	18	-36	1.1	10497+/-101		Sc	14.4	10	10		
107		375-G21	10	22	19	-36	51.5			Sb	14.4	10	6		
108		375-G22	10	22	20	-36	40.7	2749+/- 61		S0	14.0	13	11		
109		317-G23	10	22	31	-39	3.1	2892+/- 86		Sa	13.2	20	9	NGC 3244	56
110	I2575	436-G17	10	23	8	-32	22.9			S..	15.0	7	5		
111	N3244	317-G24	10	23	18	-39	34.4	2640+/-100	1	Sb-c	12.8	26	19	NGC 3244	89
112	I2576	375-G23	10	23	43	-32	38.8	9345+/- 16		Sb	14.8	8	7		
113	N3249	375-G24	10	24	7	-34	42.5	3487+/- 60		Sc	13.2	20	16	ANTLIA	6
114	N3250	317-G26	10	24	21	-39	41.3	2871+/-123	1	E	13.2	20	15	NGC 3244	83
115		375-G25	10	24	31	-36	36.5			dwarf	14.4	10	10		
116		375-G26	10	24	48	-35	58.3	3373+/- 86		Sc	13.0	23	4	ANTLIA	2
117		317-G27	10	24	49	-39	46.2			S0-a	14.2	11	2	NGC 3244	26
118		375-G27	10	24	51	-33	2.5			S..	14.4	10	5		
119		375-G28	10	25	6	-35	1.1			S0	13.8	14	4		
120	I2578	375-G29	10	25	7	-33	37.3			Sc	13.5	17	3		
121	N3250	317-G28	10	25	31	-39	44.8			Sa	13.1	22	8	NGC 3244	27
122		375-G30	10	25	32	-34	16.5			dwarf	14.4	10	5		
123	N3250	317-G29	10	25	33	-40	10.8	2520+/- 0		S..	12.8	25	8	NGC 3244	40
124		375-G31	10	25	35	-32	52.2			S..	14.4	10	4		
125	N3250	317-G30	10	25	42	-39	49.5			Sb	13.8	14	3	NGC 3244	24
126	N3251	317-G31	10	25	46	-39	33.6			Sa	13.4	18	3	NGC 3244	28
127		317-G32	10	25	52	-41	51.3			Sb	13.3	19	7		
128	I2580	436-G25	10	26	1	-31	15.8	3137+/- 20	1	Sc	12.9	24	24		
129	N3258	375-G32	10	26	4	-35	11.9			S0	14.6	9	4		
130		375-G34	10	26	9	-35	16.4			E	15.6	5	4		
131		375-G33	10	26	9	-34	13.0			Sa	14.0	13	10		
132		375-G35	10	26	21	-32	39.9			Sc	14.1	12	2		
133		436-G26	10	26	25	-30	47.0			SBa	14.4	10	6		
134	N3257	375-G36	10	26	32	-35	24.1	3023+/- 50	1	S0	14.8	8	7	ANTLIA	54
135	I2580	436-G27	10	26	36	-31	21.2	56+/- 17		S0	11.1	70	32		
136	N3258	375-G37	10	26	39	-35	21.0	2848+/- 78	1	E	13.5	17	15	ANTLIA	62
137		375-G38	10	26	47	-32	47.0			Sm	14.2	11	9		
138	N3251	317-G34	10	26	49	-39	49.6	2570+/-123		Sc	12.5	30	24	NGC 3244	82
139		375-G39	10	26	50	-36	46.6			dwarf	14.4	10	7		
140	N3260	375-G40	10	26	51	-35	20.3	2413+/- 40	1	E	14.1	12	9	ANTLIA	65
141	I2582	436-G28	10	26	52	-30	5.3			Sb	13.5	17	15		
142		375-G41	10	27	16	-35	0.2	1852+/- 37	1	S0	14.2	11	2	ANTLIA	57
143		317-G36	10	27	20	-39	35.1			S..	14.2	11	8	NGC 3244	23
144		317-G35	10	27	20	-38	47.3			dwarf	14.4	10	10		
145		317-G37	10	27	31	-41	39.1			Sa	14.4	10	7		
146		317-G38	10	27	33	-38	5.5			SB0	14.0	13	4		
147	N3267	375-G42	10	27	33	-35	4.0	3709+/- 33	1	S0	13.7	15	10	ANTLIA	33
148	I2584	375-G43	10	27	36	-34	39.3	2549+/- 57		S0	13.7	15	3	ANTLIA	70
149	N3269	375-G44	10	27	42	-34	58.0	3754+/- 33	1	Sa	12.7	27	12	ANTLIA	31
150	N3268	375-G45	10	27	45	-35	4.1	2801+/-110	1	E	13.1	22	16	ANTLIA	76
151		375-G46	10	27	50	-36	26.2			Sa-b	14.1	12	3		
152		375-G47	10	28	4	-34	8.8	3040+/- 7		Sb	13.7	15	5	ANTLIA	22
153		436-G29	10	28	5	-30	8.3	4167+/- 60	1	Sc	13.4	18	18		
154	N3271	375-G48	10	28	11	-35	6.1	3824+/- 53	1	S0	12.2	36	16	ANTLIA	25
155	N3273	375-G49	10	28	14	-35	21.2	2419+/- 52	1	S0	13.2	20	8	ANTLIA	66
156	N3275	375-G50	10	28	37	-36	28.8	3241+/-100	1	SBa	12.3	35	35		
157	I2587	375-G51	10	28	44	-34	18.4	2107+/- 66		S0	13.4	18	15	ANTLIA	39
158		375-G52	10	28	46	-36	43.1	9126+/- 47		S0	13.8	14	8		
159		317-G39	10	28	28	-39	55.3			S..	14.2	11	3	NGC 3244	17
160	N3276	317-G40	10	28	57	-39	41.3			S0-a	14.0	13	8	NGC 3244	17
161	N3258	375-G53	10	29	9	-34	57.8	2597+/-108		Sa	13.8	14	10	ANTLIA	76
162		436-G32	10	29	12	-32	27.4			S0	13.7	15	12		
163		317-G42	10	29	20	-39	18.1			E-S0	14.2	11	5	NGC 3244	5
164	N3278	317-G43	10	29	23	-39	41.9			Sc	13.7	15	12	NGC 3244	15
165		317-G44	10	29	28	-38	42.2			S..	13.7	15	6		
166	I2588	436-G33	10	29	31	-30	7.7	3562+/- 30		SBa	13.3	19	16		
167		375-G54	10	29	33	-35	46.4			Sb	13.8	14	2		
168		317-G45	10	29	35	-39	30.2			Sa	13.8	14	3	NGC 3244	9

TABLE 1 *(continued)*.

ID	NGC/IC	ESO-No.	Alpha (1950) h	m	s	Delta o	,	Rad.Vel. [km/s]	Ref.	Type	Mag.	2A [arc sec]	2B	Cluster	Probab. [%]
169	N3281	375-G55	10	29	36	-34	35.8	3549+/- 55	1	Sa-b	12.0	40	20	ANTLIA	35
170	N3259	375-G58	10	29	40	-35	9.1	2722+/- 70		Sc	13.4	18	10	ANTLIA	68
171		375-G57	10	29	40	-34	44.0			S0	14.4	10	6	ANTLIA	29
172		375-G56	10	29	40	-33	22.0			Sd	14.4	10	2		
173		375-G59	10	29	43	-34	56.4	2289+/- 22		S0	14.0	13	11	ANTLIA	69
174	N3259	375-G60	10	30	9	-34	44.5			Sm	13.3	19	4	ANTLIA	26
175		375-G61	10	30	13	-36	16.5			Sb	13.7	15	10		
176		436-G35	10	30	31	-30	0.7	3451+/- 14		Sb	13.8	14	13		
177		375-G62	10	30	32	-34	8.5			S0-a	13.8	14	2	ANTLIA	5
178	N3281	375-G63	10	30	43	-34	37.7	2779+/- 86		S0-a	13.8	14	3	ANTLIA	58
179		317-G46	10	30	49	-38	43.5			Sd	12.5	30	5		
180		317-G47	10	31	16	-41	16.3			S0	13.4	18	14		
181		436-G37	10	31	28	-31	37.5			S..	14.4	10	2		
182		317-G48	10	31	42	-39	57.1			Sd	13.7	15	14	NGC 3244	6
183		375-G64	10	31	45	-35	1.5	2573+/- 8		Sa	13.8	14	13	ANTLIA	36
184	N3289	375-G65	10	31	51	-35	3.9	2702+/- 37		Sa	12.8	26	6	ANTLIA	32
185		375-G66	10	31	54	-36	56.7			Sb	14.2	11	2		
186		375-G67	10	31	58	-35	58.5			Sd	13.7	15	3		
187	N3282	375-G68	10	32	2	-34	8.7	5366+/-108		Sb	13.1	22	4		
188		436-G40	10	32	3	-31	55.7			Sa	13.8	14	5		
189		375-G69	10	33	3	-36	37.2	3145+/- 5		S..	14.8	8	6		
190		437-G 5	10	33	14	-32	12.9			S..	13.6	16	12		
191	N3302	437-G 7	10	33	29	-32	6.0	4099+/-115		S0	13.1	22	17		
192		375-G70	10	33	34	-34	0.6	3845+/- 22		Sb	14.1	12	9		
193		375-G71	10	33	54	-36	58.7	959+/- 8	1	dwarf	11.7	50	40		
194		375-G72	10	34	22	-34	29.9			Sc	13.6	16	4		
195		437-G12	10	34	30	-30	22.1			Sb	13.8	14	11		
196		437-G14	10	34	34	-32	5.3	2840+/- 51		Sb	12.1	38	13		
197	N3318	317-G52	10	35	3	-41	22.1	2609+/- 95	1	Sc	12.6	29	16		
198		437-G16	10	35	18	-32	11.1			Sc	14.0	13	1		
199	N3318	317-G53	10	35	22	-41	12.3			Sc	13.5	17	13		
200		437-G18	10	35	32	-30	24.6			Sb	13.1	21	4		
201		317-G54	10	35	59	-37	50.4	3050+/- 5	2	Sc	12.5	30	30		
202		437-G24	10	36	6	-31	34.9			S..	14.4	10	6		
203		437-G28	10	36	26	-31	10.2			Sc	13.7	15	15		
204		437-G30	10	36	55	-30	2.3	3928+/- 86		Sc	11.9	44	8		
205		376-G 1	10	37	26	-35	1.2			Sc	13.7	15	10		
206	N3333	376-G 2	10	37	33	-35	46.5	4104+/- 24		Sb-c	13.1	22	4	NGC 3333	77
207		437-G35	10	37	44	-30	0.4			Sb	13.3	19	7		
208		376-G 3	10	37	58	-34	38.1			dwarf	13.1	21	19		
209	N3347	376-G 4	10	38	4	-36	9.1	2899+/-119		Sc	12.8	25	10		
210	N3347	376-G 5	10	38	37	-36	1.6			Sc	13.5	17	14	NGC 3333	13
211		376-G 6	10	38	50	-33	13.2			S0-a	14.0	13	4		
212		376-G 7	10	38	55	-36	53.0	4300+/- 39		E-S0	13.1	21	11	NGC 3333	79
213		318-G 3	10	39	6	-41	35.1			Sc	13.1	22	17		
214		437-G42	10	39	8	-31	31.1	2620+/- 30		SBa	12.7	28	28		
215		376-G 8	10	39	28	-36	52.9			Sb	14.2	11	3	NGC 3333	53
216		318-G 1	10	39	42	-40	0.0			Sb	14.2	11	2		
217	N3347	376-G10	10	39	43	-36	40.4			Sc	12.0	42	10	NGC 3333	60
218		376-G 9	10	39	43	-32	59.0	3058+/- 48		S0	13.3	19	4		
219		318-G 2	10	39	52	-40	18.9			Sa	13.7	15	15		
220		376-G11	10	39	54	-36	53.7			Sc	13.7	15	15	NGC 3333	52
221		376-G12	10	40	5	-35	54.9	4634+/-163		Sb	14.2	11	6	NGC 3333	43
222		437-G47	10	40	9	-30	37.4			Sc	13.5	17	8		
223		437-G48	10	40	10	-31	38.6			dwarf	14.4	10	5		
224	N3347	376-G13	10	40	29	-36	5.5	2923+/- 63	1	Sc	11.8	45	26		
225	N3354	376-G14	10	40	45	-36	6.1	2812+/- 84		S..	14.6	9	8		
226		376-G15	10	40	47	-34	38.3			Sa	14.4	10	6		
227		376-G16	10	41	10	-36	46.8			Irr	14.4	10	8	NGC 3333	13
228		437-G50	10	41	10	-30	30.6			Sb	14.1	12	8		
229		437-G51	10	41	12	-30	32.7			Sb	13.7	15	2		
230		437-G52	10	41	14	-30	22.5			S..	13.8	14	4		
231	N3358	376-G17	10	41	16	-36	8.9	2910+/-212	1	Sa-b	11.9	43	22		
232		318-G 4	10	41	34	-38	0.0	3077+/- 48		Sc	12.5	30	6		
233		437-G55	10	41	36	-30	50.7			Sa-b	14.1	12	8		
234		318-G 6	10	41	44	-39	51.4			S..	15.0	7	5		
235		437-G56	10	42	4	-31	56.8	2850+/- 68		Sb	13.2	20	14		
236		376-G18	10	42	6	-36	10.8			S..	13.8	14	9		
237		437-G59	10	42	55	-30	5.2			Sa-b	14.1	12	10		
238		376-G19	10	43	25	-36	50.0			Sc	13.7	15	3		
239		376-G20	10	44	20	-36	5.3			Sb	14.1	12	3		
240	N3378	318-G12	10	44	27	-39	45.1	5186+/- 79		Sc	13.3	19	19		
241		318-G11	10	44	27	-39	21.1			Sb	14.1	12	3		
242		318-G13	10	45	25	-38	35.4	17+/- 26		Irr	12.4	32	5		
243	N3390	437-G62	10	45	43	-31	16.1	2850+/-100	1	S0-a	11.8	45	10		
244		376-G21	10	46	1	-33	49.5			S..	13.6	16	13		
245		437-G63	10	46	40	-30	38.8			S..	14.4	10	4		
246		318-G14	10	46	51	-41	17.3			Sa	14.1	12	2		
247		437-G65	10	46	52	-31	2.4	3140+/- 33		Sa	12.7	27	12		
248		318-G15	10	47	5	-41	3.7			S..	14.4	10	1		
249		318-G16	10	47	20	-39	41.8			Sb	14.0	13	2		
250		318-G17	10	47	29	-39	35.3			SB0	14.1	12	8		

TABLE I (*continued*).

ID	NGC/IC	ESO-No.	Alpha (1950) h	m	s	Delta °	'	Rad.Vel. [km/s]	Ref.	Type	Mag.	2A [arc sec]	2B	Cluster	Probab. [%]
251		318-G19	10	48	4	-38	35.2	4765+/- 78		Sa	14.0	13	6		
252		437-G66	10	48	47	-32	3.7			S..	14.0	13	4		
253		376-G22	10	49	1	-34	9.8	1409+/- 90	1	Irr	12.9	24	6		
254		376-G23	10	49	14	-35	12.5			Sc	13.2	20	2		
255		437-G67	10	49	55	-32	24.3	3170+/- 61		SBa	12.5	30	30		
256		437-G68	10	50	2	-30	8.9			S..	14.2	11	2		
257		376-G24	10	50	19	-35	54.5			S..	13.8	14	3		
258	N3449	376-G25	10	50	32	-32	39.6	3267+/-120	1	Sb	11.7	48	12		

Ref.:

1 Lauberts (1982)

2 Huchtmeier et al. (1983)

all others : this paper

Remarks on individual Objects :

5 emission lines
20 emission lines
23 emission lines
35 Vela ring galaxy
39 OII emission line
42 OII + abs.lines
44 emission lines
48 v(Sadler)=3009km/s
57 emission lines
60 prominent emission lines
63 emission lines; abs.lines: v=(4757+/-140)km/s
64 emission lines; abs.lines: v=(4740+/-103)km/s
65 emission lines
69 only two emission lines
74 prominent emission lines
82 v(emiss.lines)=(4651+/-15)km/s
94 v(HI)=2841+-35km/s
95 v(Sadler)=2967km/s
99 emission lines, v(abs.lines)=(2637+/-161)km/s
108 emission lines
109 emission lines
113 two spectra
114 v(Sadler)=2830km/s
136 v(Sadler)=2819km/s
138 v(HI)=2818+-14km/s
150 central ellip. gal. of Antlia ,v(Sadler)=2802km/s
152 emission lines
157 v(Sadler)=2148km/s
173 emission lines
183 emission lines
189 emission lines
192 emission lines
206 emission lines, rotation curve
212 v(Sadler)=4320km/s
214 emission lines
218 v(Sadler)=3036km/s
224 v(HI)=3010+-23km/s
231 v(HI)=3010+-20km/s
247 v(HI)=3010+-20km/s

TABLE II. — *The group parameters from elliptical Gaussian fit (EG).*

		$\bar{\alpha}$	σ_α	$\bar{\delta}$	σ_δ	$\bar{v}$	σ_v	χ	μ
Antlia II	v^+	157°09	0°44	-34°98	0°31	2860.	546.	26°	20
Antlia II	v^-	157°06	0°44	-34°95	0°34	2843.	542.	14°	26
Antlia I	v^+	156°89	1°71	-35°15	0°78	2904.	456.	136°	36
Antlia I	v^-	156°96	2°67	-35°83	1°57	2817.	269.	138°	84
NGC 3244	v^+	155°74	0°55	-39°52	0°24	2725.	139.	126°	8
NGC 3244	v^-	156°24	0°71	-39°58	0°29	2719.	141.	106°	17
ESO 316-643	v^+	152°21	0°37	-38°00	0°17	4612.	280.	105°	9
ESO 316-643	v^-	152°24	0°36	-38°00	0°16	4618.	277.	105°	9
IC 2558	v^+	153°46	0°79	-34°10	0°40	2821.	252.	8°	6
IC 2558	v^-	153°01	0°53	-34°05	0°15	2740.	263.	49°	7
NGC 3333	v^+	159°70	0°51	-36°22	0°20	4333.	213.	6°	3
NGC 3333	v^-	159°92	0°37	-36°61	0°14	4425.	189.	1°	5

TABLE III. — *Distribution of the morphological types in the individual clusters.*

	E		S0		Sa-Sb		Sc-Im	
	No	%	No	%	No	%	No	%
Antlia	3	12	10	38	7	27	6	23
NGC 3244	1	5	3	16	10	53	5	26
ESO 315-G43	-	-	4	36	3	27	4	36
IC 2558	1	10	1	10	3	30	5	50
NGC 3333	-	-	1	14	2	24	4	57

TABLE IV. — *Mean radial distances to cluster center for early and late type galaxies.*

	$\langle r_{E/SO}\rangle$	$\langle r_S\rangle$
Antlia	0°42 ± 0°06	0°91 ± 0°22
NGC 3244	0°54 ± 0°15	0°76 ± 0°11
ESO 316-G43	0°37 ± 0°04	0°35 ± 0°06

TABLE V. — *Properties of the individual clusters.*

	Luminosity	Virial Radius		Mean Velocity	Velocity Dispersion	Crossing Times		Virial Mass	Mass-to-Light Ratio
	[$L_\odot$]	[degree]	[Mpc]	[km s^{-1}]		[a]	[$H_\odot^{-1}$]	[$\mathfrak{M}_\odot$]	[$\mathfrak{M}_\odot/L_\odot$]
Antlia I	$3.5\cdot10^{12}$	0.97	1.52	2828	296	$9.0\cdot10^{9}$	0.45	$9.2\cdot10^{13}$	26
Antlia II	$9.7\cdot10^{11}$	0.99	1.55	2718	469	$6.4\cdot10^{9}$	0.32	$2.4\cdot10^{14}$	243
NGC 3244	$6.1\cdot10^{11}$	1.01	1.50	2720	94	$3.1\cdot10^{10}$	1.6	$9.2\cdot10^{12}$	15
ESO 316-G43	$1.5\cdot10^{12}$	0.70	1.77	4659	294	$1.3\cdot10^{10}$	0.69	$7.7\cdot10^{13}$	73
IC 2558	$3.6\cdot10^{11}$	0.94	1.45	2702	243	$1.2\cdot10^{10}$	0.58	$6.0\cdot10^{13}$	167
NGC 3333	$1.1\cdot10^{12}$	0.75	1.77	4418	123	$2.8\cdot10^{10}$	1.4	$1.9\cdot10^{13}$	17

TABLE VI. — *Groups and clusters in the Hydra I-Centaurus supercluster.*

Name	<α> h m	<δ> ° '	<v> km s^{-1}	<v>$^{1/2}$ km s^{-1}	N	Remarks
ESO 316-G43	10 8.8	-38 0	4612.	280.	9	this paper
IC 2558	10 13.8	-34 6	2821.	252.	6	this paper
NGC 3244	10 23.0	-39 31	2725.	139.	8	this paper
NGC 3256 = Ser 77	10 26.7	-43 57	2818.	184.	4	NGC 3256, 3261, 3262, 3263
Antlia	10 28.4	-34 59	2860.	546.	20	this paper
Abell 1060 = Hya I	10 34.4	-27 16	3702.	683.		Richter (1982)
NGC 3333	10 38.8	-36 13	4333.	213.	3	this paper
NGC 3557	11 8.1	-37 4	2714.	320.	5	Sandage (1975), NGC 3557B, 3557, 3564, 3568, 3573
NGC 3606	11 13.2	-33 38	2872.		3	ESO 377-G29, -G31, NGC 3606
NGC 4373	12 26.8	-39 10	3194.	268.	6	Sandage (1975), NGC 4373, 4373A, 4507, IC 3290, 3370, ESO 322-IG 32
Centaurus	12 46.6	-41 2	3510.	870.	61	Dawe et al. (1977)
ESO 508-G19	13 6.7	-23 34	2828.	149.	4	ESO 508-G11,-G15, -G19, -G24
IC 4296	13 31.9	-33 23	3831.	199.	10	Sandage (1975), NGC 5140, 5193, 2 5220, IC 4296, 4299, ESO 383-G14, -G30, -G44, -G45, -G49
IC 4329 = Kle 27	13 46	-30 11	4478.	497.	18	Sandage (1975), Richter (1984), Klemola (1969)

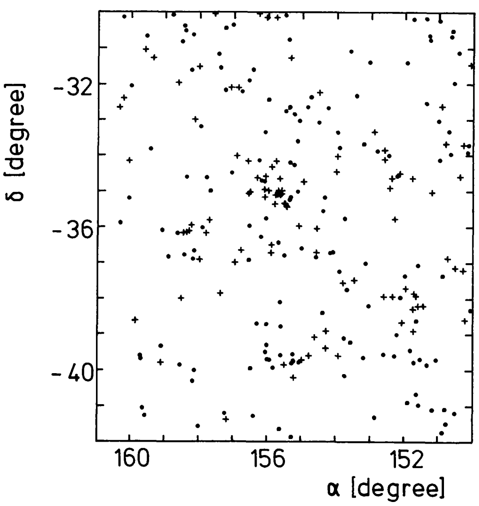

FIGURE 1. — Distribution of the galaxies of the Antlia region at the sky. Crosses indicate galaxies with measured radial velocity, dots show galaxies for which no radial velocities are known. These are all galaxies of the Lauberts catalogue in the indicated region.

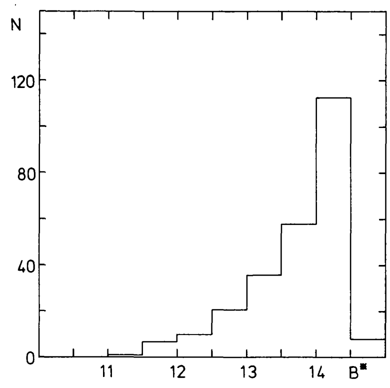

FIGURE 2. — Distribution of the galaxy magnitudes in the Antlia region. See text for the method used to derive the magnitudes B^*.

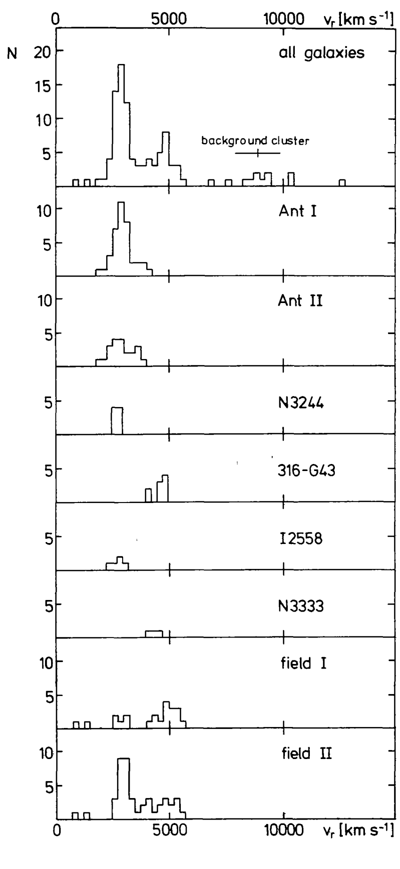

FIGURE 3. — Distribution of measured velocities for galaxies in the Antlia region. The upper most panel gives the distribution of all galaxies, the following panels for the individual clusters. Ant I is the result of the solution for the large Antlia cluster, Ant II the solution only for the central part of the Antlia cluster, cf. description in text. The two lowest panels show the distribution of the galaxies not assigned to any cluster ; « field I » is derived when the solution Antlia I is adopted and « field II » is the remainder if the solution Antlia II is taken.

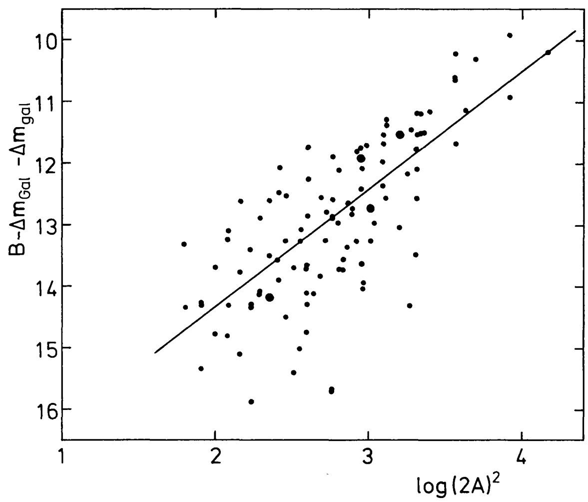

FIGURE 4. — Calibration of the B^* magnitudes. In this diagram the available B magnitudes of the Lauberts catalogue (see text for selection criteria) are plotted *versus* logarithm of the major axis squared in arc min.

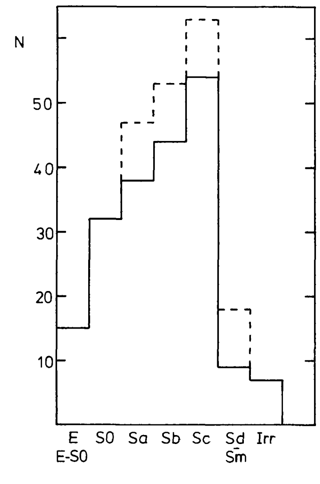

FIGURE 5. — Distribution of types of galaxies in the Antlia region. The solid line gives the galaxies with definite classification, the broken line represents also the galaxies which have only the classification S.

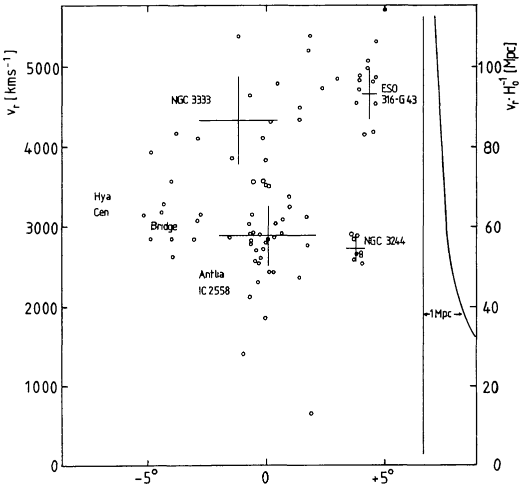

FIGURE 6. — All the galaxies with measured radial velocities in the Antlia region are plotted in a diagram radial velocity or distance *versus* position angle at the sky. The four clusters Antlia, NGC 3244, NGC 3333, and ESO 316-G43 are indicated by crosses. The horizontal bars give the size, the vertical bars the velocity dispersion. At the left the acronyms « Hya » and « Cen » indicate the mean velocities of the Hydra I and Centaurus cluster, respectively. At the right, curves are drawn to convert angles at the sky into metric distances.

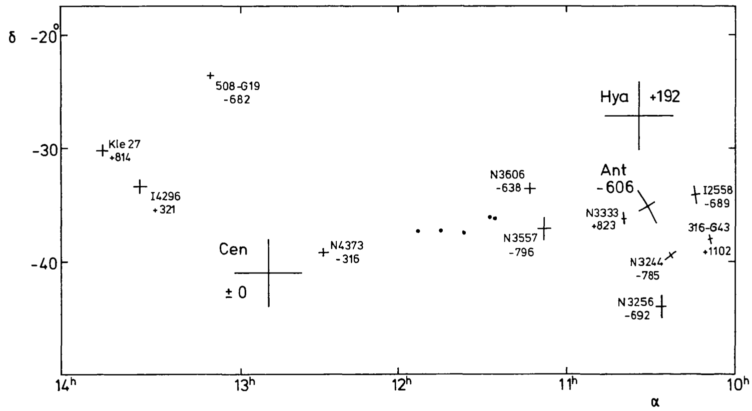

FIGURE 7. — Positions and sizes of the member clusters of the Hydra I-Centaurus supercluster are given by crosses. The inclined crosses show the position angles. In addition to names of the clusters their relative velocities with respect to the Centaurus cluster are given in km s^{-1}. The five field galaxies are indicated by dots.

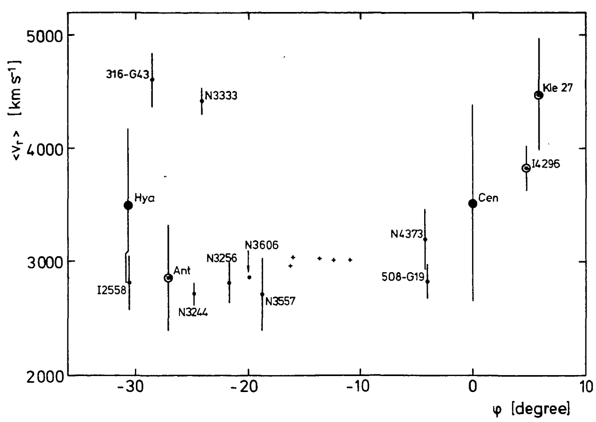

FIGURE 8. — A plot of radial velocity *versus* separation on the great circle connecting Hydra I and Centaurus for the member clusters of the Hydra I-Centaurus supercluster. Vertical bars indicate the velocity dispersion. The small crosses show the five field galaxies. The angle at the sky is counted from the Centaurus cluster along a line connecting it with the Hydra I cluster.